# A 24 GHz Flexible $10 \times 10$ Phased Array Antenna for 3D Beam Steering Based V2V Applications

Karthik Kakaraparty and Ifana Mahbub University of North Texas, Denton, Texas-76207, USA. KarthikeyaAnilKumarKakaraparty@my.unt.edu

Abstract—This paper presents a flexible  $10\times10$  phased-array antenna for efficient and high-gain 3D beam steering applications. The proposed antenna array consists of 25 quadrants of  $2\times2$  unit cells, wherein each  $2\times2$  unit cell is coaxially fed. The  $45^\circ$  phase shifting lines are incorporated in the feeding paths to facilitate the wide beamsteering range. The dimensions of the proposed phased array antenna (PAA) are  $90\times90\times0.324$   $mm^3$ . Simulation results show that the proposed phased-array antenna has a resonating frequency at 24 GHz with an operational bandwidth from 23.64 GHz to 24.31 GHz along with a high gain of 29.4 dBi. The array exhibits a maximum beam steering range of  $149.8^\circ$  in the  $\theta$  axis and  $120^\circ$  in the  $\phi$  axis with a gain variation less than 0.9 dBi. The proposed flexible PAA is suitable for its placement on curved surfaces of autonomous vehicles such as UAVs(Unmanned aerial vehicles).

Index Terms—Phased array antenna, flexible antennas, V2V applications, 24 GHz, 3D beam steering, beamforming.

#### I. INTRODUCTION

The current advancements in the wireless communications systems necessitate the efficient antenna array designs with capability of high gain and wide beam steering range. The Phased array antennas are best in achieving these goal. The PAA designs with flexible nature can facilitate the scope for many real-time applications, and this flexible nature provides opportunity to place the phased array designs even on the curved surfaces without any performance degradation. Even though there were many prior works that dealt with high frequency PAA's and the flexible antenna designs, there are very few which actually worked on optimizing the gain and enhancing the beamsteering range [1]-[11]. In this work, we present a high gain and wide beam steerable flexible PAA, suitable for its placement on curved surfaces such as on drones and on other unmanned aerial vehicles with curved surfaces. The 24 GHz band is chosen as it is license-free band and 24GHz antennas generally facilitate narrow beamwidth which makes 24 GHz band least effected with the noise interference.

The novelty of our work is that the conventional microstrip antenna array is modified by incorporating phase-shifting lines, which provides a  $45^{\circ}$  phase shift at 24 GHz to the feeding paths to enhance the wide beamsteering capability. The proposed phased array is designed to operate at 24 GHz and have dimensions of  $90\times90\times0.324~mm^3$ . Each quadrant of the whole array consists of 4 microstrip antennas that share a common coaxial feed.

The rest of the paper is organized as follows: Section II presents the antenna design methodology. In Section IV, the simulation results of the proposed PAA are discussed. Section V comprises of the concluding remarks and future works.

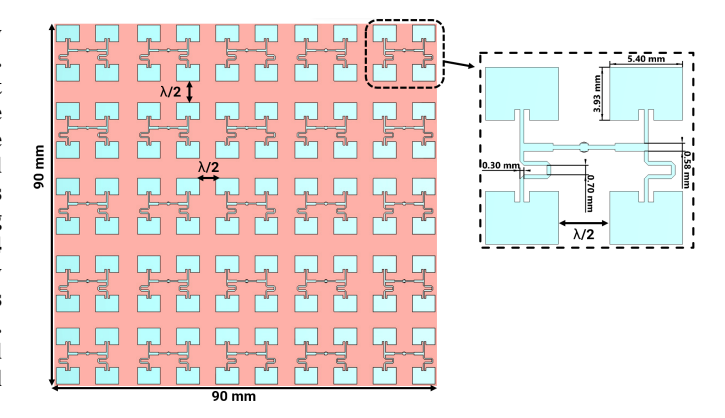


Fig. 1. The configuration of beam steering antenna array design.

#### II. ANTENNA DESIGN

The single antenna of the proposed phased array has the length and width values of  $5.40~\rm mm$  and  $3.93~\rm mm$  respectively, with feed line width of  $0.3~\rm mm$ . The antenna's substrate material is chosen as polyimide as it is light weight, highly flexible and possess high wear resistance. The dielectric constant of the substrate is 2.78. Chromium is used as a patch and the ground material as it is purported to have greater flexibility and good performance with respect to antenna gain. The configuration of the  $10\times10$  phased array is portrayed in Fig. 1. The thickness of the polyimide substrate used is  $0.254~\rm mm$  and the thickness for both the patch and the ground material individually are  $0.035~\rm mm$ . The properties of the materials used in the design are presented in Table I.

The design and simulation of the antenna array are performed using the CST (computer simulated technology) software. The whole design is divided into 25 quadrants ( $Q_1$  to  $Q_{25}$ ), wherein each  $2\times 2$  array is considered as a quadrant, and it is co-axially fed. Each quadrant is placed  $\lambda/2$  distance apart from other adjacent quadrants which ensures narrow beamwidth.

The resonating frequency considering 24 GHz, using the formula  $\lambda = v/f$ , where v is the speed of light  $(3 \times 10^8 \ m/sec)$ , the corresponding  $\lambda$  value is 12.49 mm and that of  $\lambda/2$  is 6.25 mm. The shape of the feeding lines in the antenna array design is modified by introducing a 45° phase shifter loop strip with 0.7 mm loop gap to boost the gain and to attain a wide beam steering capability in the high frequency region. Coaxial feeding is used for all ports of the antenna array in order to improve the directivity and gain.

TABLE I
MATERIALS PROPERTIES OF THE DESIGN

	Properties of Material					
Material	Permittivity $(\epsilon_r)$	Material density (kg/m <sup>3</sup> )	Young's modulus (GPa)			
Polyimide	3.5	1400.0	2.5			
Chromium	$\infty$	7190.0	140			
PTFE	2.1	2200.0	0.575			

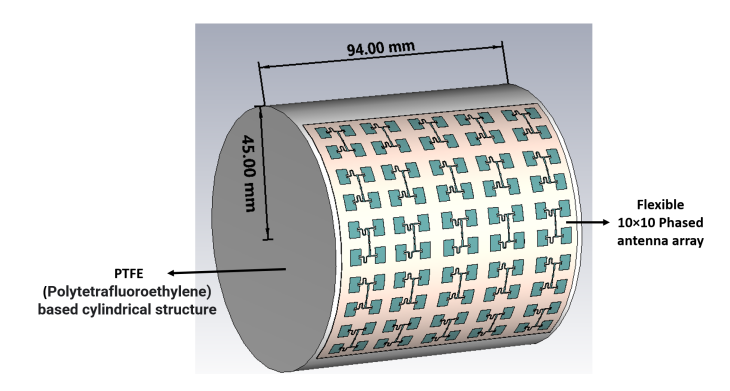


Fig. 2. Flexible  $10 \times 10$  PAA wrapped on a cylindrical surface.

As shown in Fig. 2, the flexible PAA is wrapped on a curved cylindrical structure and the material used for this structure is PTFE (PolyTetraFluoroEthylene) which is a synthetic polymer commonly used for making drones and wings of unmanned aerial vehicles. Each quadrant of the proposed PAA is coaxially fed. The designed cylindrical structure has a radius of 45 mm and a height of 94 mm. the The S-parameter performance of the designed flexible PAA which is wrapped on to the surface of cylindrical structure is tested to analyze its performance capability.

# III. Envisioned Fabrication Procedure

The proposed PAA is intended to be fabricated with utilization the concept of photo-lithography. The concept of photo-lithography is illustrated in Fig. 3 (a) and the fabricated photomask is presented in Fig. 3 (b). The photomask is fabricated for the proposed  $10 \times 10$  PAA design with help of CAD/Art Services, Inc., a leading supplier of high-quality photomasks and phototools. A negative photo-resist based photo-lithography technique is suitable for fabricating this proposed PAA. The polyimide substrate is first coated with the chromium with a 0.035 mm thickness utilizing the Electron-beam physical vapor deposition (EBPVD) procedure. This coated sample is undergone through the photo-lithography procedure, in which the coated sample is covered with the fabricated photomask and is exposed to UV (Ultra violet) light as presented in the Fig. 3 (a).

The fabricated photomask has the black portion which is not transparent and as a result the UV light cannot penetrate through it and on the other hand, transparent regions are the ones which make up the whole 10 PAA design, as as shown in the Fig. 3 (b), which allow UV light to pass through and thus the photoresist which is exposed to UV light is retained

and the region of photo-resist that is not exposed to UV light is removed after etching and development stage.

### IV. RESULTS AND DISCUSSION

The simulated  $S_{11}$  parameter result for the single antenna element,  $10 \times 10$  PAA and  $10 \times 10$  array when placed on curved body are shown in the Fig. 4. The magnitude value of the  $S_{11}$  (in dB) for each antenna element at resonating frequency is -40 dB and that of the  $10 \times 10$  PAA is -39.45 dB, both indicating the good resonance at the desired resonating frequency which is 24 GHz. For the case where the  $10 \times 10$  PAA is wrapped on the cylindrical structure, the magnitude value of the  $S_{11}$  (in dB) is -29.5 dB. This is because the effective dielectric constant of the substrate changes when in contact with PTFE based cylindrical surface.

A comparative analysis has been carried out between the simulation results of the  $10 \times 10$  PAA, and array of 100 antennas each individually fed. The 45° phase shifting microstrip lines incorporated in the feeding paths of each quadrant facilitated the wide beamsteering capability of the proposed PAA. The Fig. 5 portrays the farfield simulation results for array of 100 antennas each element with a separate coaxial feed, Fig. 5 (a) presents the beam scanning range of -57.5° to 58° along the  $\theta$  axis and Fig. 5 (b) presents the scanning range of 0° to 70.5° along  $\phi$  axis. The simulation results of the proposed PAA demonstrate a wide scanning range of -74.8° to 75° along the  $\theta$  axis and 0° to 120.5° in  $\phi$  axis as shown in the Fig. 6 (a) and Fig. 6 (b) respectively. The gain variations in the both aforementioned scenarios is less than 0.9 dBi.

The proposed PAA provides a highest gain of 29.3 dBi with a operating bandwidth of 23.64 GHz to 24.31 GHz, with resonating frequency at 24 GHz. The acheived narrow beamwidth value of the proposed PAA is 19.5° in the  $\theta$  axis. The beam steering and gain values for different input phases for proposed  $10 \times 10$  PAA are tabulated in Table II and the results for the considered scenario where array of 100 antennas with an array factor of  $10 \times 10$  (each antenna is individually fed using coaxial feed technique), are tabulated in Table III. The comparision of the proposed work with prior published works is presented in Table IV. When compared to the considered prior works, even though the size of proposed antenna is comparable, the proposed PAA showed a better widebeam steering capability due to the incorporation of phaseshifting lines in the feeding paths. The proposed PAA has also shown better performance with respect to narrow beam width and high gain.

The proposed antenna array is flexible and has a high gain value of 29.3 dBi along with 149.8° wide beam steering capability along the  $\theta$  axis. The  $10\times10$  PAA has demonstrated wide beam steering and more focused beam with beamwidth value of 19.5°, when compared to array with 100 antennas without any phase shifters incorporated in the design. This indicate that the PAA has the better performance capability with respective to narrow beamwidth and wide beam steering capability when compared to the individually fed antenna elements.

Fig. 3. Beamsteering and gain values along  $\theta$  axis and  $\phi$  axis for  $10 \times 10$  PAA for different input phases at 24 GHz.

	Theta (θ)		Gain		Phi (ф)		Gain
Q1-Q25	Beam Direction	HPBW	(dBi) Q1-Q25	Q1-Q25	Beam Direction	HPBW	(dBi)
-120°	-74.8°	19.5°	29.4	-60°	00	20.2°	29.1
-60°	0°	19.8°	29.2	30°	60°	19.7°	28.7
00	75°	20.1°	28.9	60°	120.5°	20.3°	28.4

Fig. 4. Beamsteering and gain values along  $\theta$  axis and  $\phi$  axis for array of 100 antennas for different input phases at 24 GHz.

	Theta (θ)		Gain		Phi (ф)		Gain
Q1-Q25	Beam Direction	HPBW	(dBi)	Q1-Q25	Beam Direction	HPBW	(dBi)
-120°	-57.5°	26.1°	28.4	-60°	00	23.2°	28.3
-60°	00	25.4°	28.2	30°	35°	24.4°	28.1
00	58°	24.9°	27.9	60°	70.5°	23.7°	27.6

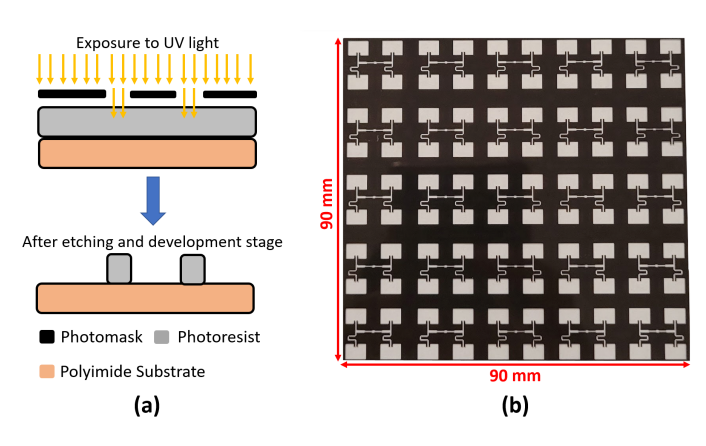


Fig. 5. Microfabrication process (a) Photo-lithography process with negative photo-resist (b) Fabricated photomask.

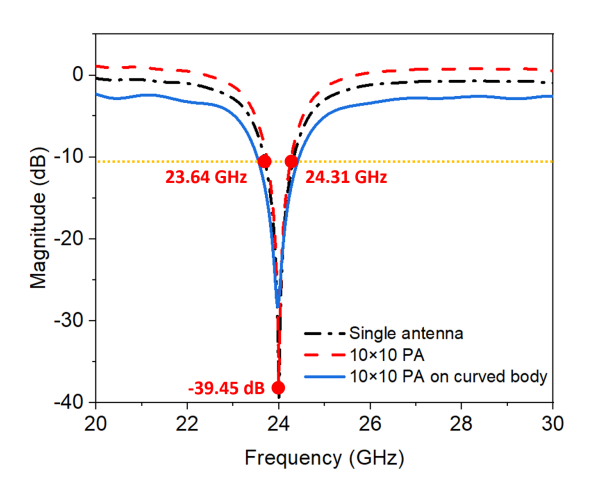


Fig. 6.  $S_{11}$  parameter result.

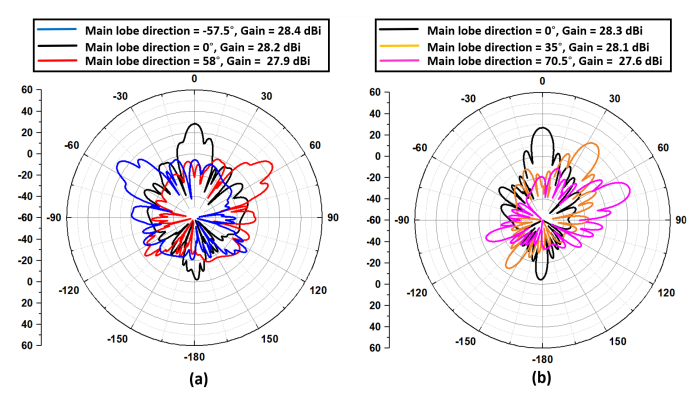


Fig. 7. Far-field directivity of the array of 100 antennas (a) In  $\theta$  axis (b) In  $\phi$  axis for different input signal phase at 24 GHz.

The S-parameter simulation results of the single antenna element,  $10 \times 10$  PAA and the case when PAA is placed on curved body showed good agreement with each other. The flexible PAA when wrapped on curved cylindrical structure gave a reliable S-parameter results, showing the resonance at 24 GHz which is the desired frequency of operation. The simulated farfield radiation patterns indicate that the proposed PAA is highly directional, with the beamwidth values ranging from as low as  $19.5^{\circ}$  to as high as  $20.3^{\circ}$ . The farfield directivity results presented in Table III are for the 100 antenna elements arranged with an array dimensions of  $10 \times 10$  and each antenna element is fed coaxially. The farfield directivity results were analyzed for difference input phases at resonating frequency which is 24 GHz.

The scenario where all antenna elements fed individually showed the wider beamwidth values ranging from as low as  $23.2^{\circ}$  to as high as  $26.1^{\circ}$ . The case where the quadrant approach is implemented, where in each  $2\times 2$  is quadrant that has single co-axial feed, with the phaseshifting lines

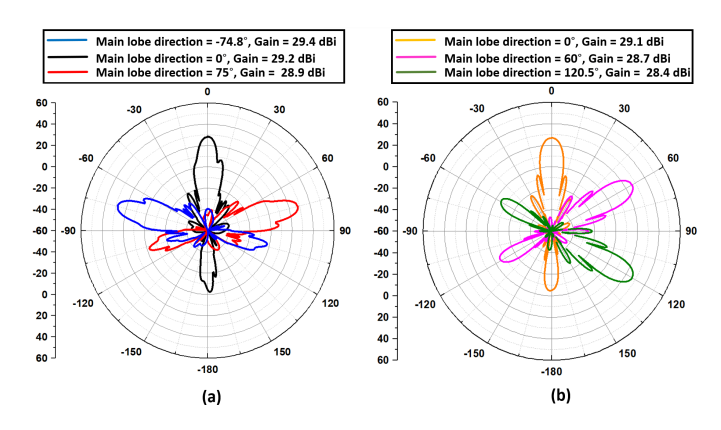


Fig. 8. Far-field directivity of the  $10 \times 10$  PAA (a) In  $\theta$  axis (b) In  $\phi$  axis for different input signal phase at 24 GHz.

# TABLE II COMPARISON WITH OTHER WORKS

	[12]	[13]	[14]	This Work*
Array factor	$1 \times 4$	$1 \times 16$	1 × 8	10 × 10
Operating frequency (in GHz)	24	24	28	24
Array Gain (in dBi)	6.17	14.43	16.3	29.4
Beam Steering range	90°	10°	100°	EP:149.8°, AP:120°
Size mm <sup>2</sup>	$27.56 \times 53$	$104 \times 7$	$60 \times 100$	90×90
Beam-angle	60°	20°	24°	19.5°

<sup>\*</sup> This work is based on simulation

incorporated in the design has shown better performance with respect to narrow beam width, high gain and wide beam steering capability.

#### V. CONCLUSION

A compact 25 port co-axially fed PAA is presented that is suitable for 3D beamsteering applications. The high gain value of 29.3 dBi, with a wide beamsteering capability of 149.5° along the  $\theta$  axis and 120° along the  $\phi$  axis portray the good performance capability of the proposed antenna. The resonating frequency value for all the three considered scenarios are in good agreement with each other, which shows the reliability of the proposed  $10\times10$  PAA. As a future work, we plan to utilize the fabricated photomask to fabricate the proposed  $10\times10$  PAA to analyze the measured and simulation performance results.

#### ACKNOWLEDGMENT

This work is based upon work supported by the National Science Foundation (NSF) under Grant No. ECCS 2148178.

## REFERENCES

- [1] K. Hu, X. He, and M. M. Tentzeris, "Flexible and scalable additively manufactured antenna array tiles for satellite and 5g applications using a novel rugged microstrip-to-microstrip transition," in 2021 IEEE International Symposium on Antennas and Propagation, 2021, pp. 37–38.
- [2] B. Yan, W. Sheng, C. Shi, J. Lu, and H. Xu, "Wideband wide-scanning phased array of u-slot microstrip antenna elements in triangular lattice," in 2019 IEEE International Symposium on Phased Array System Technology (PAST), 2019, pp. 1–5.
- [3] A. Samaiyar, P. V. Prasannakumar, M. A. Elmansouri, L. Boskovic, D. S. Filipovic, and S. Rao, "Phased array antenna for bi-static simultaneous transmit and receive (star) systems," in 2019 IEEE International Symposium on Phased Array System Technology (PAST), 2019, pp. 1–5.

- [4] J. Zhang, W. Chang, and J. Zheng, "Study on different array allocation for simultaneous transmit and receive used in phased array," in 2019 IEEE International Symposium on Phased Array System Technology (PAST), 2019, pp. 1–5.
- [5] D. You, D. Awaji, A. Shirane, H. Sakamoto, and K. Okada, "A flexible element antenna for ka-band active phased array satcom transceiver," in 2020 IEEE Asia-Pacific Microwave Conference (APMC), 2020, pp. 991–993.
- [6] D. Busuioc and S. Safavi-Naeini, "Low-cost antenna array and phased array architectures — design concepts and prototypes," in 2010 IEEE International Symposium on Phased Array Systems and Technology (PAST), 2010, pp. 965–968.
- [7] H. Chen and R. Gentile, "Phased array system simulation," in 2016 IEEE International Symposium on Phased Array Systems and Technology (PAST), 2016, pp. 1–6.
- [8] O. S. Mizrahi, A. Fikes, and A. Hajimiri, "Flexible phased array shape reconstruction," in 2021 IEEE MTT-S International Microwave Symposium (IMS), 2021, pp. 31–33.
- [9] L.-J. Chen and M.-J. Yan, "Design of 24ghz microstrip phased array antennas with low side-lobe," in 2016 IEEE International Conference on Electronic Information and Communication Technology (ICEICT), 2016, pp. 606–608.
- [10] W. F. Moulder, R. N. Das, A. C. Maccabe, L. A. Bowen, E. M. Thompson, and P. J. Bell, "Rigid-flexible antenna array (rfaa) for lightweight deployable apertures," in 2020 14th European Conference on Antennas and Propagation (EuCAP), 2020, pp. 1–5.
- [11] J. Yang, H. Zhang, H. Luo, X. Shen, and Z. Mo, "Application of flexible degradation technology to phased-array antenna," in 2021 2nd China International SAR Symposium (CISS), 2021, pp. 1–3.
- [12] N. Kathuria and B. C. Seet, "24 ghz flexible lcp antenna array for radar-based noncontact vital sign monitoring," in 2020 Asia-Pacific Signal and Information Processing Association Annual Summit and Conference (APSIPA ASC), 2020, pp. 1472–1476.
- [13] F. Suliman and A. Yazgan, "24 ghz patch antenna array design with reduced side lobe level for automotive radar system," 2020 28th Signal Processing and Communications Applications Conference (SIU), pp. 1– 4, 2020.
- [14] A. Khabba, S. Ibnyaich, and M. M. Hassani, "Beam-steering millimeterwave antenna array for fifth generation smartphone applications," 2019 International Conference of Computer Science and Renewable Energies (ICCSRE), pp. 1–5, 2019.